

New insights into upper MOW variability over the last 150 kyr from IODP 339 Site U1386 in the Gulf of Cadiz



Stefanie Kaboth^{a,*}, André Bahr^b, Gert-Jan Reichart^{a,c}, Bram Jacobs^a, Lucas J. Lourens^a

^a Department of Earth Sciences, Faculty of Geosciences, Utrecht University, Heidelberglaan 2, 3584 CS Utrecht, The Netherlands

^b Institute of Earth Sciences, Ruprecht-Karls-Universität Heidelberg, Im Neuenheimer Feld 234, 69120 Heidelberg, Germany

^c Royal Netherlands Institute for Sea Research (NIOZ), P.O. Box 59, AB Den Burg, 1790 Texel, The Netherlands

ARTICLE INFO

Article history:

Received 18 February 2015

Received in revised form 8 July 2015

Accepted 24 August 2015

Available online 1 September 2015

Keywords:

Mediterranean outflow

Glacial–interglacial variability

Sapropel

Heinrich events

Gulf of Cadiz

ABSTRACT

The upper Mediterranean Outflow Water (MOW) paleo-oceanographic history in the Gulf of Cadiz is poorly constrained due to the lack of high-resolution records that pre-date the last glaciation. Existing proxy records concentrate on MOW variability along the middle slope of the Gulf of Cadiz. Here we present a continuous high-resolution benthic foraminifera $\delta^{18}\text{O}$ record from the upper MOW core at IODP Expedition 339 Site U1386 in the Gulf of Cadiz of the past 150,000 years. Based on $\delta^{18}\text{O}$, grain-size and Zr/Al variability comparison of our results with existing Mediterranean Sea (MD01–2472, MD95–2043), open ocean (LR04) and Gulf of Cadiz (MD99–2339) records we have gathered new insights into the evolution of the upper MOW core on glacial–interglacial timescales. The influence of the upper MOW at Site U1386 was strongest during MIS 5 and MIS 1. Similar $\delta^{18}\text{O}$ variability can be seen in the Levantine Intermediate Water (LIW) originating from the Levantine Basin of the Eastern Mediterranean Sea. We found clear indication for a vertical shift of the MOW from the upper to the middle slope of the Gulf of Cadiz during sea level lowstands coinciding with MIS 4 and MIS 2 but also during MIS 3. Additionally, our results indicate an increased upper MOW flow correlated with Heinrich Events 7 to 10 and the Younger Dryas, and also inversely relate to precession-forced monsoonal freshwater inputs into the Eastern Mediterranean. In the context of Sapropel formation, we could not find conclusive evidence of the proposed MOW shutdown in our data.

© 2015 The Authors. Published by Elsevier B.V. This is an open access article under the CC BY-NC-ND license (<http://creativecommons.org/licenses/by-nc-nd/4.0/>).

1. Introduction

Mediterranean Outflow Water (MOW) is an end-member of the thermohaline exchange between the Mediterranean Sea and the adjacent North Atlantic Ocean, providing a source for warm, highly saline water to the eastern North Atlantic through the Gibraltar Gateway (Baringer and Price, 1999; Bersch et al., 2007; Bryden et al., 1994; Hernández-Molina et al., 2014; Iorga and Lozier, 1999; Thorpe, 1976) (Fig. 1A). The present-day Atlantic–Mediterranean exchange through the Gibraltar Gateway is driven by the evaporation loss of the Mediterranean Sea itself (Bryden et al., 1994; Sankey, 1973). This results in the inflow of colder and less-dense North Atlantic water at the surface and the outflow of warmer and denser Mediterranean sourced water masses at depth (Ambar and Howe, 1979; Bryden and Stommel, 1984; Bryden et al., 1994) (Fig. 1A). The outflowing water masses consist predominately (~70%) of Levantine Intermediate Water (LIW), formed in the Eastern Mediterranean Basin, and changeable parts of Western Mediterranean Deep Water (WMDW) originating in the Alboran and Tyrrhenian Sea (Millot, 2009, 2014; Millot et al., 2006). Upon leaving the Strait of

Gibraltar, the MOW plume cascades down and follows the seafloor morphology of the Gulf of Cadiz, while penetrating northwest along the continental slope (Ambar and Howe, 1979; Hernández-Molina et al., 2006, 2014; Mulder et al., 2006) overlying North Atlantic Deep Water (NADW), and underlying North Atlantic Central Water (NACW) and Antarctic Intermediate Water (AIW) (Baringer and Price, 1999; Hernández-Molina et al., 2014). As a water mass, the MOW can be traced within the Gulf of Cadiz in two major flow cores located at 800–1400 m water depth alongside the middle slope (lower MOW core), and at 500–700 m water depth alongside the upper slope including our study area (upper MOW core, Fig. 1B) (Baringer and Price, 1997; Borenäs et al., 2002; Hernández-Molina et al., 2013).

Since the reopening of the Strait of Gibraltar at 5.3 Ma (Hernández-Molina et al., 2014; Maldonado and Nelson, 1999) the Gulf of Cadiz is a key area to study MOW variability on glacial–interglacial time scales as its contourite depositional system has been shaped under the direct influence of the MOW (Hernández-Molina et al., 2006, 2014; Llave et al., 2006, 2007; Nelson et al., 1993, 1999; Schönfeld and Zahn, 2000; Schönfeld, 1997; Stow et al., 2002; Toucanne et al., 2007; Voelker et al., 2006).

Previous studies have demonstrated the sensitivity of the upper and lower MOW core to climatic forcing on diverse time scales (e.g. Bahr

* Corresponding author.

E-mail address: S.Kaboth@uu.nl (S. Kaboth).

et al., 2014; Llave et al., 2006, 2007; Nelson et al., 1993, 1999; Rogerson et al., 2005; Schönfeld and Zahn, 2000; Schönfeld, 1997; Siirro et al., 1999; Toucanne et al., 2007; Voelker et al., 2006). A variable spatial MOW influence was considered on glacial–interglacial timescales. It was argued that the lower MOW core was enhanced during cool (sea level lowstand) periods, favoring the development of sandy contourites whereas during warm climatic periods (sea level highstand) sandy contourites developed in shallower areas where the upper MOW was enhanced (Hernández-Molina et al., 2006; Llave et al., 2006, 2007; Schönfeld and Zahn, 2000; Voelker et al., 2006; Zahn et al., 1987). To explain this apparent pattern, an approximate doubling of the settling depth of the MOW plume during glacial periods was suggested due to increased density (Rogerson et al., 2005, 2012; Schönfeld and Zahn, 2000). On millennial time scales, evidence was found that North Atlantic Climate Oscillations such as Heinrich Events (HE1 to HE6) caused a short-term strengthening of the MOW alongside the upper and middle slope (Llave et al., 2006; Schönfeld and Zahn, 2000; Schönfeld, 2002; Toucanne et al., 2007; Voelker et al., 2006). In addition, it was argued that the absence of MOW would reduce the Atlantic Meridional Overturning Circulation by as much as 15% compared to modern (Rogerson et al., 2006). The lack of sufficient long sediment records has so far hampered a full understanding of MOW variability on orbital and millennial timescales but also the assessment of its global impact. This is changing now rapidly with the Plio/Pleistocene contourite drift sequences retrieved during IODP Expedition 339 from the Gulf of Cadiz (Hernández-Molina et al., 2013; Stow et al., 2013).

In this paper, we present a new benthic foraminifera oxygen isotope and a grain-size record from IODP 339 Site U1386 located on the upper slope of the Gulf of Cadiz (Fig. 1B). In an integrated approach, we correlate our data to existing Mediterranean Sea, open ocean and Gulf of Cadiz records (Fig. 1B). We aim to relate our data to glacial–interglacial induced sea level variations, Heinrich Events (HEs) and Sapropel (S) formation in the Eastern Mediterranean Sea. This study is a contribution to deepen our understanding on how these climatic oscillations affected upper MOW variability at Site U1386 in the past, how upper MOW core variations relate to changes in the lower MOW core at the same time, and how hydrographic changes within the Mediterranean Sea contributed to these variations over the last 150 kyr.

2. Material & methods

2.1. Site U1386

Integrated Ocean Drilling Program (IODP) Site U1386 was drilled during Expedition 339 in November to January 2011/2012 and is located southeast of the Portuguese Margin mounded on the Faro Drift along the Alvarez Cabral Moat at 36°49.68'N; –7°45.32'W in 561 m water depth (Fig. 1B and C). The Faro drift is part of the Contourite Depositional System (CDS) of the Gulf of Cadiz (Stow et al., 2013). At present, IODP Site U1386 is directly influenced by the upper MOW core (Hernández-Molina et al., 2013; Stow et al., 2002, 2013). The composite depth scale (meters composite depth, MCD) was developed from parallel holes at Site U1386 during the expedition (Hernández-Molina et al., 2013), and has been applied in this study. For this study 161 sediment samples were analyzed for $\delta^{18}\text{O}$ and grain-size at 30 cm intervals between 0 to 45.08 MCD (~150 kyr) resulting in an approximately 1 kyr resolution.

2.2. Oxygen isotopes

The freeze-dried sediment samples were wet sieved into three fractions: (>150 μm , >63 μm and >38 μm), and their residues oven dried at 40 °C. Stable oxygen isotope analyses were carried out on 4 to 6 specimens of the epifaunal living foraminifera species *Planulina ariminensis* from the >150 μm size fraction. All selected specimens were crushed, sonicated in ethanol, and dried at 35 °C. Stable isotope analyses were

carried out on a CARBO-KIEL automated carbonate preparation device linked to a Finnigan MAT253 mass spectrometer at Utrecht University. The precision of the measurements is $\pm 0.08\text{‰}$ for $\delta^{18}\text{O}$. The results were calibrated using the international standard NBS-19, and the in-house standard NAXOS. Isotopic values are reported in standard delta notation (δ) relative to the Vienna Pee Dee Belemnite (VPDB).

Changes in the $\delta^{18}\text{O}$ of foraminifera reflect a combination of global ice volume (sea level), temperature and local hydrographic influences such as salinity (Hodell et al., 2010). For our site-to-site comparison (see Section 2.6) one can assume that the global ice volume contributions within the same time frame for the different $\delta^{18}\text{O}$ records are equal. Consequently, differences in $\delta^{18}\text{O}$ are caused by temperature and/or salinity differences of the water masses at the different sites. With this approach we are able to utilize $\delta^{18}\text{O}$ as a water mass tracer for MOW variability at Site U1386.

2.3. X-ray fluorescence analyses

The geochemical composition of sediment from Site U1386 was analyzed using a XRF Core Scanner II, (AVAATECH Serial No. 2) at the Royal Netherlands Institute for Sea Research (NIOZ). XRF scanning provides semi-quantitative estimates of light atomic weight (e.g. aluminum) to heavy elements such as barium in a nondestructive manner (Jansen et al., 1998; Richter et al., 2006). XRF Core Scanner data were collected every 1 cm down-core over a 1.2 cm² area with down-core slit size of 10 mm in three separate runs using generator settings of 10, 30, and 50 kV, and a current of 1.5 mA respectively. Sampling time was set to 10, 20 and 40 s respectively and scanning took place directly at the split core surface of the archive half. The split core surface was covered with a 4 μm thin SPEXCerti Prep Ultralene1 foil to avoid contamination of the XRF measurement unit and desiccation of the sediment. The data were acquired by a Canberra X-PIPS Silicon Drift Detector (SDD; Model SXD 15C-150–500) with 150 eV X-ray resolution and the Canberra Digital Spectrum Analyzer DAS 1000. Raw data spectra were processed with the Iterative Least square software (WIN AXIL) package from Canberra Eurisys. To account for XRF signal distortions such as porosity variations, sediment surface roughness and the formation of a water film from condensation below the covering foil we “normalized” the raw total counts of a given element to the total counts of all processed elements for the same measurement position. This step of “normalization” reduces signal artifacts related to pronounced lithological changes (Bahr et al., 2014). The relative standard deviations of selected element counts for Site U1386 are aluminum (Al) = 1.43%, bromine (Br) = 3.57% and zirconium (Zr) = 1.45%.

2.4. Grain-size analyses

The oxygen isotope sample preparation was used to obtain weight percentages of the grain-size fractions >150 μm , 150–63 μm , 63–38 μm and <38 μm for every sample. We concentrate on the grain-size fraction between 63 and 150 μm which has been used previously as indicator for flow strength changes in the Gulf of Cadiz attributed to MOW variability (Rogerson et al., 2005). We disregard the size-fraction >150 μm to reduce the bias caused by planktic and benthic foraminifera abundances and test-size as well as IRD contributions.

To further account for the possible carbonate bias in the weight percentage of the size-fraction 63–150 μm we visually correlated these results to the Zr/Al ratios derived from the XRF scanning of the sediments. Bahr et al. (2014) argued that the Zr/Al ratio mainly reflects bottom current velocity and accumulation of heavy minerals linked to MOW variability.

2.5. Age control

Our chronology is based on the tuning of normalized bromine (Br) (Br/total counts) at Site U1386 derived from XRF scanning (Fig. 2;

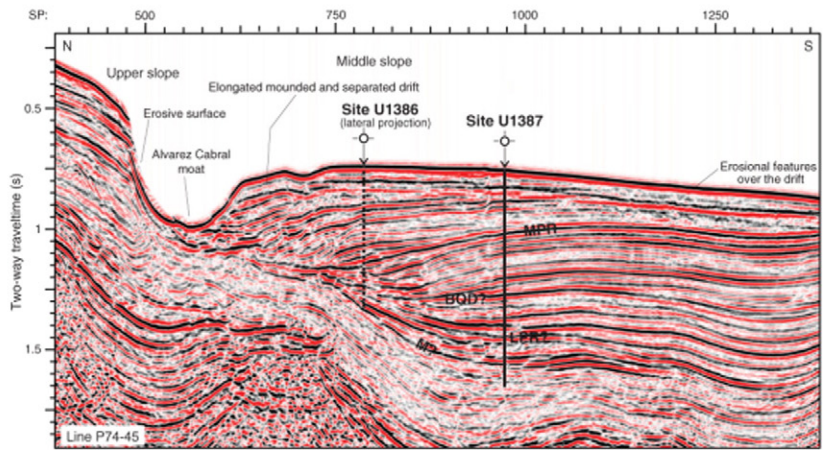
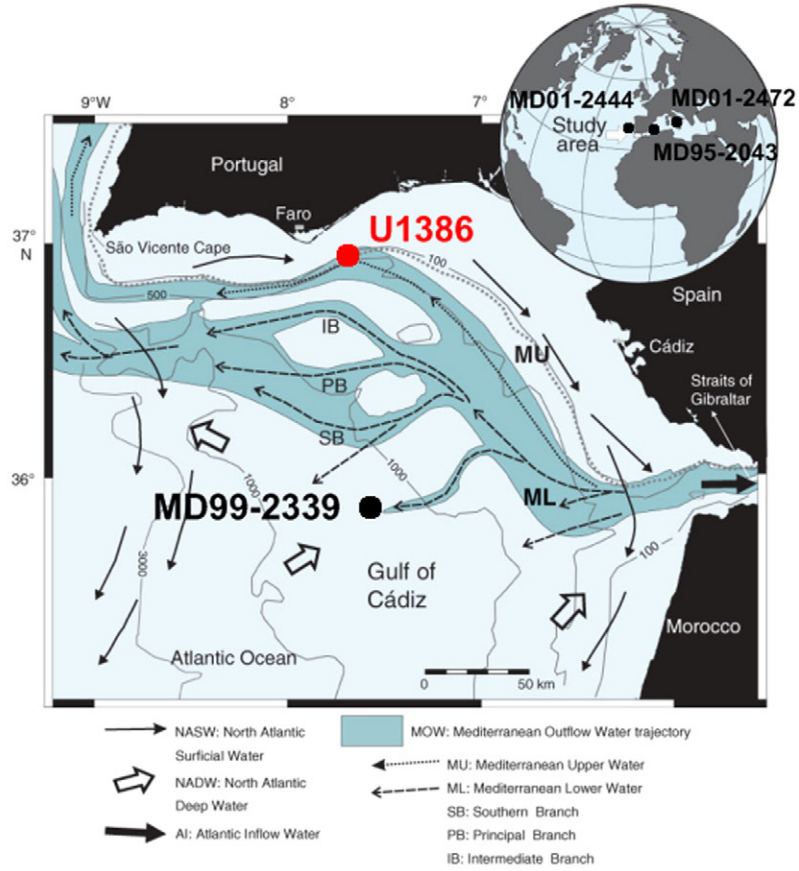
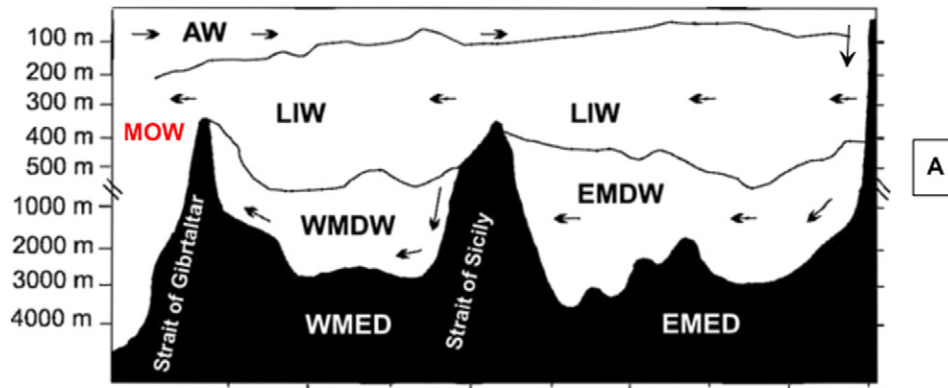


Table 2A and B) to the planktonic *G. bulloides* $\delta^{18}\text{O}$ record from core MD01-2444 (Barker et al., 2011; Hodell et al., 2013). This approach follows Bahr et al. (2014) who showed that conditions at the sea surface drive the Br content at Site U1387 which is located in vicinity and similar water depth as Site U1386 (Fig. 1C, Hernández-Molina et al., 2013). It was argued that Br is not distinctly influenced by varying lithology and its variations are not directly linked to other elements, making it an excellent tool for stratigraphic correlation (Bahr et al., 2014).

The chronology of the Marine Isotope Stages (MIS) follows Lisiecki and Raymo, 2005. Heinrich Events (HEs) were identified following Sanchez Goñi and Harrison, 2010 for HE1-6. The timing of the HE1-6 in the Hodell et al. (2013) chronology slightly differs from the GICC05 based chronology applied by Sanchez Goñi and Harrison (2010). Following their description of the relationship of HEs and Greenland Stadials/Interstadials (GS/GI) we adapted their ages to our chronology. Following Bahr et al. (2014), the older HE 7-11 are based on the correlation of $\delta^{18}\text{O}$ and SST records of Site MD01-2444 (Martrat et al., 2007) put on the age model of Hodell et al. (2013). Heinrich Events 7 to 11 correspond to Iberian Margin Stadial (IMS) periods 1-IMS21, 22, 24, 25 and 2-IMS-1, respectively.

2.6. Site-to-site comparison of $\delta^{18}\text{O}$

To evaluate changes in Mediterranean Outflow influence at Site U1386 during the last 150 kyr, we compared the $\delta^{18}\text{O}$ record from Site U1386 in the Gulf of Cadiz to the $\delta^{18}\text{O}$ records of cores MD01-2472 (Toucanne et al., 2012), MD99-2339 (Voelker et al., 2006) and MD95-2043 (Cacho et al., 2006) (Fig. 1B, Table 1). MD01-2472 is located at the Corsica Through (Northern Tyrrhenian Sea, Western Mediterranean) and bathes today in Levantine Intermediate Water (LIW). MD95-2043 is located in the western Alboran Sea within the Western Mediterranean Deep Water (WMDW) mass. WMDW is in addition to LIW the main contributor to MOW (Millot, 2009; Millot et al., 2006; Rogerson et al., 2012). MD99-2339 is located in the Eastern Gulf of Cadiz within the lower core of the MOW (Voelker et al., 2006).

For our comparison, we first corrected the four $\delta^{18}\text{O}$ records for interspecies offsets. For this purpose, we followed the calibration of Shackleton and Hall, 1984, who showed that *Uvigerina* spp. reliably represents calcite $\delta^{18}\text{O}$ in equilibrium with the ambient water mass, therefore setting the baseline for our comparison. The isotope record of core MD01-2472 is based on *Uvigerina* spp. therefore no further adjustment was necessary (Toucanne et al., 2012). The $\delta^{18}\text{O}$ records of cores MD95-2043 and MD99-2339, which are mainly based on *Cibicides* spp., were adjusted to those of *Uvigerina* by adding 0.64‰ to the $\delta^{18}\text{O}$ values following Shackleton and Hall (1984) (see also Cacho et al., 2006; Voelker et al., 2006). Our oxygen isotope record of Site U1386 is based on *P. ariminensis*. Zahn et al., 1987 showed a small offset of -0.3‰ for $\delta^{18}\text{O}$ between *P. ariminensis* and *Cibicides wuellerstorfi*. To align Site U1386 to cores MD01-2472, MD99-2339 and MD95-2043 we adjusted the $\delta^{18}\text{O}$ values first to *C. wuellerstorfi* by -0.3‰ following Zahn et al. (1987), and secondly to *Uvigerina* by adding 0.64‰ following Shackleton and Hall (1984).

3. Results

3.1. Normalized Br and chronology

Normalized Br values (Br/total counts) at Site U1386 range between -0.07 and -0.02 within the time period investigated in this study. The

highest values correlate to the early Holocene and the lowest values to late MIS 5. Despite the lack of an inherent glacial–interglacial pattern there is a good signal correlation on millennial and sub-millennial timescales between Br and planktonic *G. bulloides* $\delta^{18}\text{O}$ record from core MD01-2444 (Barker et al., 2011; Hodell et al., 2013; Martrat et al., 2007), as previously described by Bahr et al. (2014) (Fig. 2A).

However, the comparison of the $\delta^{18}\text{O}$ record of Site U1386, based on our age model, to LR04 (Lisiecki and Raymo, 2005) based on its respective age model yields a distinct offset between the records at the penultimate transition TII (~ 130 kyr) (Fig. 2C). This is not surprising since the LR04 stack, contrary to the absolute “Speleo-Age” timescale of MD01-2444 published by Hodell et al. (2013) and based on Barker et al. (2011), contain inherent assumptions about the time lag between insolation forcing and ice-sheet response (Hodell et al., 2013).

To qualitatively investigate TII time offset further we included the SST record of core MD01-2444 from the Iberian Margin based on its initial age model which is based on the GICC05 and EDC2 chronology (Martrat et al., 2007). Note, that the SST record was not used for the purpose of constructing our chronology.

The comparison of these three records, each drawn on their individual age scales, yields a good agreement for TI and obvious differences at TII (Fig. 2E). It seems feasible that the application of MD01-2444, based on the age scale of Hodell et al. (2013), as tuning target introduced the TII offset into our $\delta^{18}\text{O}$ record in comparison to LR04 and the SST record. This comparison showcases that independently from the age model used a TII offset would have occurred in comparison to LR04. Without better constraint at TII from possible tuning targets we are at this point unable to further validate our tuning for this time interval. As a consequence we exclude from our discussion TII and the preceding MIS6.

The estimated mean sedimentation rate for Site U1386 (Fig. 2D) is ~ 0.4 m/kyr which differs from the relatively uniform sedimentation rate of ~ 0.25 m/kyr that has been calculated from shipboard stratigraphy for the past 1.8 Myr (Hernández-Molina et al., 2013; Stow et al., 2013). For the lower slope of the Gulf of Cadiz, Voelker et al. (2006) showed sedimentation rates between 0.3 and 0.5 m/kyr. However, average sedimentation rates do not fully characterize the history of accumulation. A doubling and tripling of the sedimentation rate coincides with the transition of MIS 5 to MIS 4 (~ 75 ka) and TI (~ 10 ka). Condensed sections with low sedimentation rates of <0.1 m/kyr correlate with two intervals at ~ 70 kyr and 75 to 85 kyr, respectively.

3.2. Oxygen isotopes

Fig. 2 shows the comparison between our $\delta^{18}\text{O}$ record of U1386 with the global mean $\delta^{18}\text{O}$ stack LR04 (Lisiecki and Raymo, 2005). The good signal correlation of these records for the last 150 kyr highlights the ice volume induced glacial–interglacial variability at Site U1386 (Fig. 2C).

On glacial–interglacial timescales Site U1386 shows lightest values (-1.20 – -1.30‰) during interglacials MIS 5 and 1 and glacial enrichment in $\delta^{18}\text{O}$ (-3.33 – -3.17‰) during MIS 4 and MIS 2. The penultimate transition TII and the last termination TI show depletion of -2.32‰ and -1.90‰ , respectively. In comparison, MIS 3 is ambiguous showing a mixed glacial/interglacial behavior (see Fig. 2C).

While the $\delta^{18}\text{O}$ signal of Site U1386 and LR04 are coherently in-phase, $\delta^{18}\text{O}$ amplitude variations between these two signals are visible especially during MIS 5 and MIS 1 (Fig. 2C). These periods at Site U1386 are marked by a series of millennial-scale oscillations of

Fig. 1. Study area and Mediterranean Sea circulation (A) simplified East–West cross section showing water mass circulation in the Mediterranean Sea (modified after Elshaway et al., 2010). WMED = Western Mediterranean Sea; EMED = Eastern Mediterranean Sea; NASW = North Atlantic Surface Water; LIW = Levantine Intermediate Water; EMDW = Eastern Mediterranean Deep Water; WMDW = Western Mediterranean Deep Water; MOW: Mediterranean Outflow Water. (B) Location map of the Gulf of Cadiz showing the recent flow pattern of MOW modified after (Hernández-Molina et al., 2013; Stow et al., 2013); site locations of U1386 (upper MOW core, this study), MD99-2339 (lower MOW core, Voelker et al., 2006), MD95-2043 (Alboran Sea, Cacho et al., 2006) and MD01-2472 (Corsica through, Mediterranean Sea, Toucanne et al., 2012) are marked. (C) Multichannel seismic (MCS) reflection profile (Line P74-45) of Sites U1386 and U1387 on the Faro-Drift (MCS lines provided by REPSOL Oil Company). SP = shot point. MPR = mid-Pleistocene revolution discontinuity, BQD = base quaternary discontinuity, LPR = intra-lower Pliocene discontinuity, M = late Miocene discontinuity (Hernández-Molina et al., 2013).

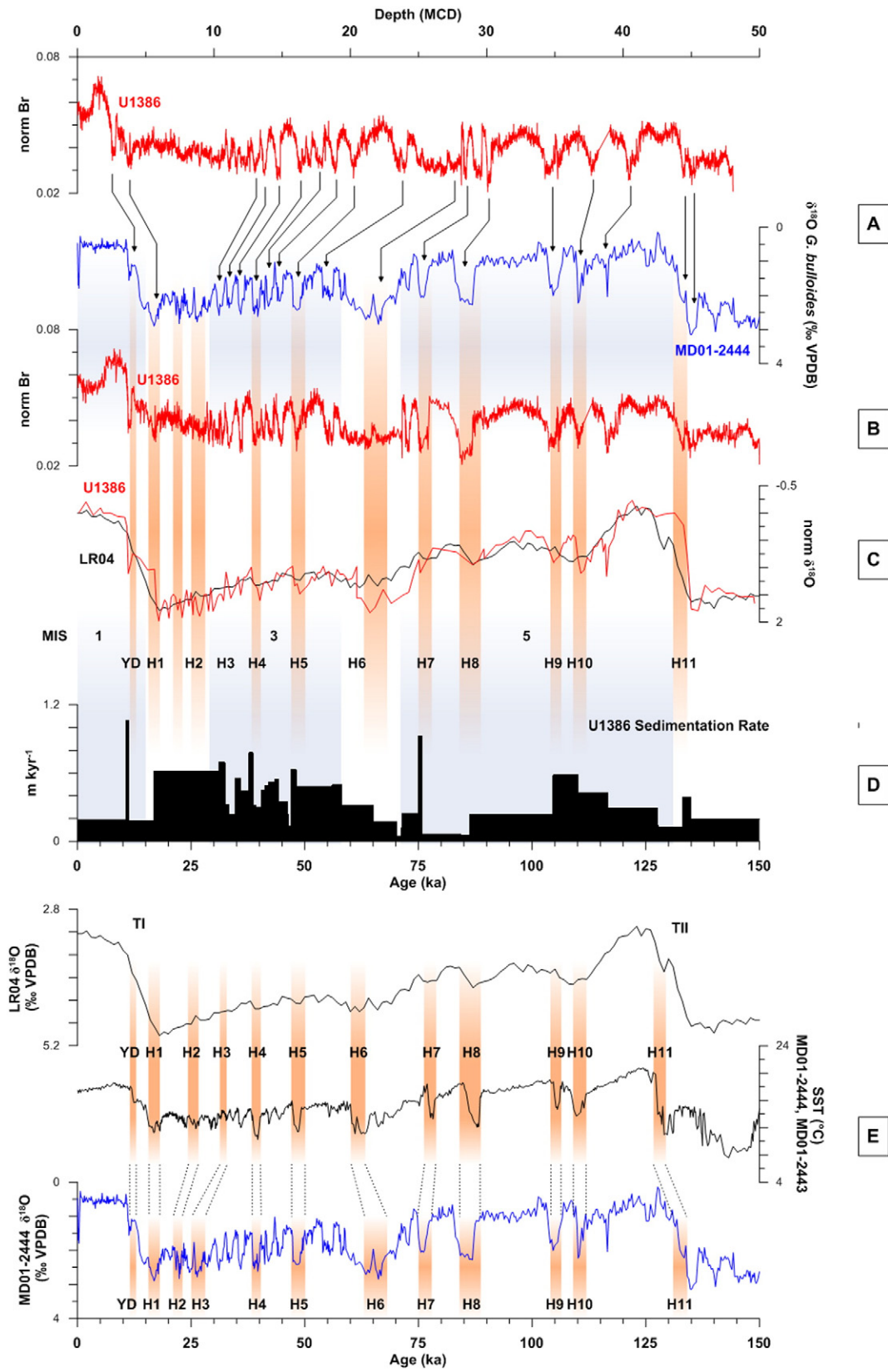


Table 1

Coordinates, water depth and corresponding water mass of used sites for $\delta^{18}\text{O}$ and grain-size comparison (Fig. 1B).

Site	Lat (N)	Lon	Water depth (m)	Water mass
U1386	36°49.68	7°45.32 W	561	Upper MOW ¹
MD01-2472	42°36.42	9°43.97 E	501	LIW ²
MD99-2339	35°52.80	7°31.80 W	1170	Lower MOW ³
MD95-2043	36°8.58	2°37.26 E	1841	WMDW ⁴

¹ This study.

² Toucanne et al., 2012.

³ Voelker et al., 2006.

⁴ Cacho et al., 2006.

triangular shape coinciding with Heinrich Events (HE7–HE10 during MIS 5) (following Bahr et al., 2014), Iberian Margin Stadials (20–25 during MIS 5) (Martrat et al., 2007), and the Younger Dryas (MIS1). These perturbations are of the order of up to 0.5‰ (e.g. MIS 5e) compared to the global mean $\delta^{18}\text{O}$.

3.3. Grain-size and Zr/Al ratios

In general, the highest grain-size values (63–150 μm) of >15wt.% occur during interglacials MIS 5 and MIS 1 but are, with the exception of the late Holocene, correlated to the same short term variability observed in our $\delta^{18}\text{O}$ record (Fig. 3A). Highest values of up to ~33wt.% are correlated with MIS 5d. The lowest grain size values correspond to glacial periods MIS 4 and MIS 2 with values <5wt.% (63 μm). The grain-size values during MIS 3 show, similar to the $\delta^{18}\text{O}$ values, a mixed glacial/interglacial character.

The Zr/Al ratio at Site U1386 (see Fig. 3A) shows a similar glacial–interglacial behavior as the grain-size values (Fig. 3A). Highest Zr/Al values (4.7 to 7.6) are linked to the same short-term variability observed in the grain-size values during MIS 5 and MIS 1. The weight percentages of 63–150 μm record mimics the Zr/Al signal at Site U1386.

4. Discussion

4.1. Glacial–interglacial MOW variability

Site U1386 reveals similar $\delta^{18}\text{O}$ values as MD01-2472 during MIS 5e and MIS 1 (Fig. 3A). This correspondence emphasizes the direct influence of LIW variability on upper MOW and its influence at Site U1386 during these time intervals, similar to modern conditions. During the alternating full glacial periods MIS 4 and MIS 2, LIW is characterized by enriched $\delta^{18}\text{O}$ values at MD01-2472 relative to Site U1386. This results in a clear $\delta^{18}\text{O}$ gradient (gray shaded area in Fig. 3A) between these two locations, suggesting that at Site U1386 is no longer influenced by the upper MOW core and bathys in more open ocean waters during these glacial time periods. A reduced isotopic gradient between both sites during MIS 5d to MIS 5a and MIS 3 points furthermore to the absence or a substantially reduced MOW influence during these time intervals at Site U1386.

In the context of glacial periods, our findings corroborate the outcome of previous studies of the last glaciation that show a reduction in

Table 2

Age control points used for the construction of the chronology at Site U1386 based on alignment of the normalized Br counts at Site U1386 to the planktic $\delta^{18}\text{O}$ Record of the Iberian Margin core MD01-2444 (Barker et al., 2011; Hodell et al., 2013) (Fig. 2A and B).

Depth (MCD)	Age (ka)
0	0
2	10.642
2.7	11.302
3.7	16.831
12.5	31.12
13.4	32.419
13.7	33.341
14	34.64
14.7	35.902
15.5	37.702
16.2	38.6
16.4	39.23
16.75	40.401
17.1	41.178
17.5	41.995
18.2	43.33
18.7	44.249
19.4	46.25
19.5	47
20.2	48.11
24	56
25	58
27.21	65.037
28.05	70
28.1	71.24
29	74.95
29.55	75.544
30.05	84.194
30.15	86.174
34.5	104.6
37.7	110.11
40.45	116.53
43.7	127.6
44.4	133.12
45.04	134.77
48.05	150

the upper MOW branch activity while the lower MOW limb increases in flow, i.e. an approximate doubling of the settling depth of the MOW plume (Rogerson et al., 2005, 2012; Toucanne et al., 2007; Voelker et al., 2006). The downslope shift of the MOW plume during glacials was related to the reduced cross-section of the Gibraltar–Gateway in combination with the glacial induced increase in salinity of the Mediterranean Sea itself (Hernández-Molina et al., 2006; Rogerson et al., 2012). Numerical simulations, however, indicate that the MOW flow speed within the Strait of Gibraltar does not change significantly in response to sea-level variations (Alhammoud et al., 2010). An increased salinity due to the lowered sea level during MIS 5d to 5a and MIS 3 compared to MIS 5e and MIS 1 could explain the increased isotopic gradient (Fig. 3A), and might also indicate a downslope shift of a denser MOW during these intervals.

To test the downslope shift of MOW during MIS 3 and MIS 2 we included the $\delta^{18}\text{O}$ record of piston core MD99-2339 from the middle slope of the Gulf of Cadiz (Voelker et al., 2006) into our comparison. MD99-

Fig. 2. Chronology of Site U1386; Blue columns represent MIS stages. Orange columns indicate Heinrich Events (H). Termination I and II are indicated by TI and TII, respectively and follow the chronology Lisiecki and Raymo (2005). (A) Normalized Br record of Site U1386 on shipboard MCD scale correlated to the planktonic $\delta^{18}\text{O}$ (*G. bulloides*) from core MD01-2444 (Barker et al., 2011; Hodell et al., 2013). The chronostratigraphy of MD01-2444 follows Hodell et al. (2013) which is based on tuning of the $\delta^{18}\text{O}$ record to the synthetic Greenland ice core of Barker et al. (2011). Lines with arrows indicate selected tie points used for the age model (a full list of tie points is available in Table 2). (B) Normalized Br record of Site U1386 on new time scale according to our tuning. (C) Comparison of the normalized benthic $\delta^{18}\text{O}$ record of Site U1386 on new time scale according to our tuning, and normalized global mean $\delta^{18}\text{O}$ LR04 stack on its respective age model (Lisiecki and Raymo, 2005). (D) Calculated Sedimentation rate for Site U1386. (E) Comparison of the planktic $\delta^{18}\text{O}$ record of MD01-2444 (blue line, Barker et al., 2011; Hodell et al., 2013), the SST record of MD01-2444, MD01-2443 (Martrat et al., 2007) and LR04 (Lisiecki and Raymo, 2005), on their respective age models. The correlation of Heinrich Events (brown columns) and Terminations I–II is shown between the different age chronologies.

2339 is argued to have been influenced by the lower MOW branch during the last 50 kyr (Voelker et al., 2006). During late MIS 3 and MIS 2 the $\delta^{18}\text{O}$ signal at MD99-2339 is slightly depleted relative to the $\delta^{18}\text{O}$ signal at MD01-2472 (Fig. 3B). This might be due to admixing of $\delta^{18}\text{O}$ depleted inflowing North Atlantic Surface Water (NASW) into the MOW during its passage through Gibraltar. The isotopic gradient related to MD01-2472 is smaller than the gradient between U1386 and MD01-2472 at the same time indicating a downslope shift of MOW during this interval, and are consistent with our initial findings of a reduced upper MOW influence at Site U1386 (Fig. 3B). During MIS 1, the isotopic gradient increases substantially between MD99-2339 and MD01-2472 while the gradient between U1386 and MD01-2472 reduces, coinciding with the proposed increase of upper MOW flow during the late Holocene (Bahr et al., 2014; Llave et al., 2006; Rogerson et al., 2005).

At first these results seem to contradict the findings of Bahr et al. (2014) where the observed MIS 3 variability at Site U1387, located in the vicinity of Site U1386 (Fig. 1C), was attributed to MOW variability. However, Site U1386 is located closer to the present day upper MOW flow core. With lowered sea-levels during MIS 3, and inferred denser MOW than compared to MIS 1 and MIS 5e, it is possible that the upper MOW core was vertically shifted downward influencing Site U1387 instead of Site U1386.

To explain the increased density of MOW during MIS 3 and MIS 2 Voelker et al. (2006) showed a close correlation between the $\delta^{18}\text{O}$ signal of MD99-2339 and the $\delta^{18}\text{O}$ record of MD95-2043 (Fig. 1B) from the Gulf of Lions (Cacho et al., 2006) on millennial and sub-millennial timescales. MD95-2043 is thought to show changes in Western Mediterranean Deep Water (WMDW) (Cacho et al., 2006). Based on the $\delta^{18}\text{O}$ signal correlation as well as the $\delta^{13}\text{C}$ comparison of MD99-2339 and MD95-2043 it was argued that WMDW contributions to MOW increased during MIS 3 and MIS 2 (Voelker et al., 2006). The comparison between MD99-2339, MD95-2043 and MD01-2472, within the error margin of the individual age models, shows that LIW is also characterized by very similar MIS 3 variability, and is relatively enriched in $\delta^{18}\text{O}$ (Fig. 3B). It is therefore possible that a denser LIW, due to the lowered sea level induced salinity increase, instead of WMDW, increased MOW density supplying the lower MOW core during MIS 3 and MIS 2.

4.2. Millennial-scale MOW variability

The grain size (63–150 μm) and Zr/Al records of Site U1386 do not show a distinct glacial–interglacial pattern corresponding with the $\delta^{18}\text{O}$ variability. The highest grain-size and Zr/Al values occur during interglacials MIS 5 and MIS 1 but are, with the exception of the late Holocene, correlated to sub-millennial high-latitude North Atlantic Climate Oscillations such as Heinrich Events (HE) 10 to 7, Greenland Stadials (GS) 20–25 and the Younger Dryas (YD) (Fig. 3A).

On millennial timescales, a coherent relationship between Greenland temperatures and grain size variability in the Gulf of Cadiz was revealed for lower MOW core records, available only during the interval HE6 to HE1 (Cacho et al., 1999; Rogerson et al., 2012; Voelker et al., 2006). It was shown that Heinrich Events correspond to relatively high energy MOW periods and enhanced sand deposition on the middle slope of the Gulf of Cadiz (Rogerson et al., 2005; Toucanne et al., 2007; Voelker et al., 2006). Llave et al. (2006) also recognized HE1, HE2, HE4 and HE6 as horizons depicted with coarse terrigenous debris in the upper MOW branch. At Site U1386 grain-size (63–150 μm) and Zr/Al ratios are also increased during the YD, while HE6 to HE2 are devoid of coarser grains. The interval during HE6 to HE1 coincides with an absent or less enhanced upper MOW influence at Site U1386 which may account for a bias in the grain-size data during this interval. For Site U1387 increased upper MOW flow was also suggested during HE10 to HE1 and the YD (Bahr et al., 2014).

It is noteworthy that the grain-size and Zr/Al variability at Site U1386 seems to be highly sensitive to millennial scale variations during sea level highstands and interglacials MIS 5 and MIS 1. Moreover, a

decreasing trend in grain-size (63–150 μm) variability from MIS 5e to 5a, coinciding with lowering sea levels, and an increasing trend from the early MIS 1 to the late MIS 1, coinciding with increasing sea levels, can also be seen.

During HE6 to HE1 (MIS 4–2) when sea level was lower than compared to MIS 5 and MIS 1, Voelker et al. (2006) suggested an increased entrainment of WMDW into the MOW, facilitated by the colder temperatures over the Western Mediterranean Sea. This was argued to explain the increased flow speed along the middle slope. This argument could also be used during HE10 to HE7 (MIS 5) at Site U1386 where an increased entrainment of WMDW into a less dense interglacial MOW could increase the flow strength of the upper MOW core and therefore account for our results during these time periods. It was also argued that changes of the MOW settling depth not only relate to the characteristics of its source water masses but also the degree of mixing with ambient North Atlantic water masses as well as their vertical structure in the Gulf of Cadiz (Llave et al., 2006; Rogerson et al., 2012). Rogerson et al. (2012) emphasized the latter especially for periods of sluggish North Atlantic Deep Water (NADW) formation; such is the case during Heinrich Events. However, these time intervals also coincide with repeated short-lived enrichments in $\delta^{18}\text{O}$ at Site U1386 and at MD01-2472 suggesting a density increase of LIW feeding into the MOW at the same time.

4.3. Sapropel formation and its influence on upper MOW variability

Sapropels are a distinct sedimentary feature of the Eastern Mediterranean Sea coinciding with periods of precession-induced strong monsoonal rain fall in northern Africa (Cramp and O'Sullivan, 1999; Rossignol-Strick, 1985; Ziegler et al., 2010). These periods coincide with maxima in low latitude summer insolation during precession minima, driving the northward expansion of monsoonal rain belts. Amplified freshwater discharge into the Eastern Mediterranean Sea reduced intermediate and deep water convection, and is argued to have disrupted the North Atlantic–Mediterranean Sea exchange through the Gibraltar gateway causing a reduction in MOW formation, as documented for the Holocene Sapropel 1 (S1) in the Gulf of Cadiz (Cramp and O'Sullivan, 1999; Meijer and Tuenter, 2007; Myers et al., 1998; Rogerson et al., 2012; Rossignol-Strick, 1985; Toucanne et al., 2007; Voelker et al., 2006).

For more insight on the possible precession control on upper MOW variability, we compared the $\delta^{18}\text{O}$ records of U1386 and MD01-2472 with the Chinese composite Sanbao and Hulu cave $\delta^{18}\text{O}$ speleothem record (Wang et al., 2008, Fig. 3A). This record shows East Asian Monsoon activity which is dynamically linked to the African Monsoon system (Yamamoto et al., 2013). Depleted $\delta^{18}\text{O}$ values of the Sanbao–Hulu record have been related to maximum intensity of the African monsoon coinciding with an increase in precipitation and river run off over the Eastern Mediterranean Sea (Fig. 3A; Ziegler et al., 2010).

In this context, the $\delta^{18}\text{O}$ signal comparison of Site U1386 and MD01-2472 is particularly interesting since MD01-2472 is directly recording LIW variability originating from the Eastern Mediterranean Basin (Toucanne et al., 2012). During sapropel formation, a freshwater induced reduction of intermediate and deep-water circulation in the Eastern Mediterranean Basin, leading to a reduced MOW, would decrease the supply of denser and therefore isotopically heavier water masses at Site U1386 (see Fig. 3A). We would expect Site U1386 to become more influenced by the open ocean signal and hence appear relatively depleted in $\delta^{18}\text{O}$ compared to MD01-2472, with the isotopic gradient between these two sites increasing. This is the case for S4 and S3 where the $\delta^{18}\text{O}$ of MD01-2472 is enriched and remains relatively depleted at Site U1386. In contrast, S5 and S1 show a decreased isotopic gradient between these sites. The lowered sea-level during MIS 5c and MIS 5a corresponding to S4 and S3 compared to S5 and S1 (MIS 5e and MIS 1) could account for these deviations since the expected salt accumulation during S4 and S3 had a more prominent effect.

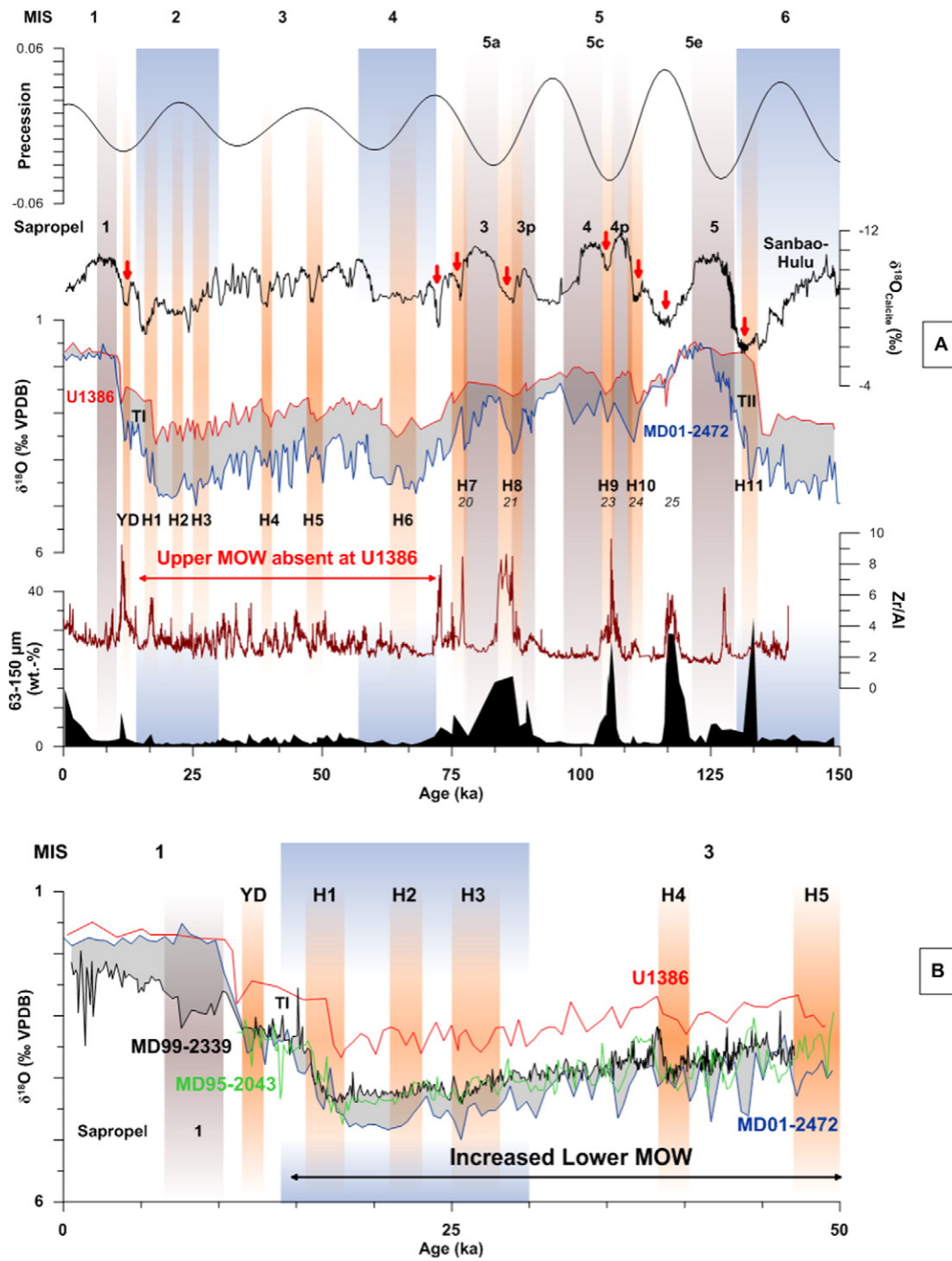


Fig. 3. Orbital and millennial scales induced MOW variability over the last 150 kyr. Blue columns represent MIS stages. Orange columns indicate Younger Dryas (YD), Heinrich Events (H) and Greenland Stadials 20 to 25 (italic). Brown columns representing Sapropel (S) following the chronology of Ziegler et al., 2010. Termination I and II are indicated by TI and TII, respectively and follow the chronology Lisiecki and Raymo (2005). (A) Comparison of Precession derived from the astronomical solution of La2010 (Laskar et al., 2011), Sanbao-Hulu $\delta^{18}O$ speleothem record (Wang et al., 2008), normalized $\delta^{18}O$ of sites U1386 (upper MOW core, red line, this study) and MD01-2472 (Levantine Intermediate Water, blue line, Toucanne et al., 2012) over the last 150 kyr including the grain-size (63–150 μm) and Zr/Al records from Site U1386. Small red arrows indicate intervals of inverse relationship to precession-forced monsoonal freshwater input into the Eastern Mediterranean. (B) Comparison of $\delta^{18}O$ records from Site U1386 (upper MOW core, red line, this study), MD01-2472 (Levantine Intermediate Water, blue line, Toucanne et al., 2012), MD99-2339 (lower MOW core, orange line, Voelker et al., 2006) and MD95-2043 (Western Mediterranean Deep Water, green line, Cacho et al., 2006) over the last 50 kyr.

Empirical reconstructions and modeling also suggest that thermally driven (Myers, 2002) remnant overturning circulation still occurs even throughout the most extreme surface freshening phases (De Lange et al., 2008; Meijer and Tuenter, 2007; Myers et al., 1998; Rogerson et al., 2012). If true, this argues against a complete collapse of Eastern Mediterranean Sea circulation since LIW formation could still occur;

with surface water masses remaining dense enough for intermediate water formation even if deep water formation was halted. This could argue for the formation of a relatively less dense and $\delta^{18}O$ depleted LIW (or better, its equivalent at that time) in the Eastern Mediterranean Sea, creating a less dense MOW which then less vigorously interacted with the Gulf of Cadiz sediments after passing the Gibraltar Gateway.

This scenario might also explain the lack of sandy contourite on the middle slope within the Gulf of Cadiz (Toucanne et al., 2012; Voelker et al., 2006). The displacement of LIW comparable to present day by intermediate water masses depleted in $\delta^{18}\text{O}$ at MD01-2472 during S5 and S1 might also explain our observations.

For the Holocene S1, the proposed reduction of MOW is documented by the absence of sandy contourite layers from the middle slope of the Gulf of Cadiz at MD99-2339 (Voelker et al., 2006) and MD99-2431 (Toucanne et al., 2007). Based on the low grain size values coinciding with decreased magnetic susceptibility Voelker et al. (2006) argued a sudden reduction in flow strength and sediment delivery by the lower MOW core towards MD99-2339 during this time interval, as only an increased bottom flow strength would facilitate an increased deposition of ferromagnetic, lithic grains (Voelker et al., 2006). Toucanne et al., 2007 also argued a flow reduction coinciding with Sapropel 1 at MD99-2341, located on the central slope, based on low grain size values. It was argued that the general inactivity of MOW lead also to the deposition of muddy contourites on the upper slope causing a Gulf-wide “Holocene sandy contourite gap” (Rogerson et al., 2012). The grain-size and Zr/Al values at Site U1386 show slightly increased values during the early phases of S5, and S3p, but are typically low throughout intervals of sapropel formation.

Interestingly, the high amplitude grain-size (63–150 μm) and Zr/Al variations at Site U1386 occurring in-between S4p and S4 and S3p and S3 are inversely related to precession-forced monsoonal freshwater input into the Eastern Mediterranean while also coinciding with high latitude cold events HE8 and HE7 (indicated by small red arrows in Fig. 3A). This relationship is not limited to the intervals of S4 and S3 but also present at Site U1386 throughout MIS 5 and MIS 1. Reduced riverine freshwater input into the Levantine Basin might have caused intense intermediate water formation promoted by the intrusion of cold and dry air masses into the Eastern Mediterranean related to a strong Siberian High as inferred for the Younger Dryas and Heinrich Events (Kotthoff et al., 2008), and could have enhanced the upper MOW against the background of global ice volume change.

5. Conclusions

Our results from Site U1386 suggest a direct influence of the upper MOW during MIS 5e and MIS 1 suggesting LIW to be the main contributor to MOW; these circumstances resemble modern conditions. During the glacial sea-level lowstands the Upper MOW core did not supply Site U1386 due climate paced modification of LIW creating a denser and deeper flowing MOW. During MIS 5d to 5a and MIS 3 the Upper MOW influence at Site U1386 seems to be also reduced or completely absent. Our results suggest that a certain sea level threshold is required for MOW to increase its influence Site U1386.

Grain-size and Zr/Al variability at Site U1386 seems to be highly sensitive to sub-millennial scale variations at Site U1386 during sea level highstands and interglacials MIS 5 and MIS 1 correlating with North Atlantic Cold Events as well as reduced riverine input during reduced Monsoon activity.

Acknowledgments

We thank two anonymous reviewers for providing helpful suggestions for the improvement of the final version of this paper. We acknowledge the Integrated Ocean Drilling Program (IODP) for providing the samples used in this study as well as A. van Dijk at Utrecht University and R. Gieles at NIOZ for analytical support. This research was funded by NWO-ALW grant (project number 865.10.001) and Lucas J. Lourens. We thank T. Kouwenhoven and F. Hilgen for providing valuable comments on the manuscript.

References

- Alharmoud, B., Meijer, P.T., Dijkstra, H.A., 2010. Sensitivity of Mediterranean thermohaline circulation to gateway depth: a model investigation. *Paleoceanography* 25, PA222. <http://dx.doi.org/10.1029/2009PA001823>.
- Ambar, I., Howe, M.R., 1979. Observations of the Mediterranean outflow—II the deep circulation in the vicinity of the Gulf of Cadiz. *Deep Sea Res. Part A* [http://dx.doi.org/10.1016/0198-0149\(79\)90096-7](http://dx.doi.org/10.1016/0198-0149(79)90096-7).
- Bahr, A., Jiménez-Espejo, F.J., Kolasinac, N., Grunert, P., Hernández-Molina, F.J., Röhl, U., Voelker, A.H.L., Escutia, C., Stow, D.A.V., Hodell, D., Alvarez-Zarikian, C.A., 2014. Deciphering bottom current velocity and paleoclimate signals from contourite deposits in the Gulf of Cadiz during the last 140 kyr: an inorganic geochemical approach. *Geochemistry, Geophys. Geosystems* 15, 3145–3160. <http://dx.doi.org/10.1002/2014GC005356>.
- Baringer, M.O., Price, J.F., 1997. Mixing and spreading of the Mediterranean outflow. *J. Phys. Oceanogr.* [http://dx.doi.org/10.1175/1520-0485\(1997\)027<1654:MASOTM>2.0.CO;2](http://dx.doi.org/10.1175/1520-0485(1997)027<1654:MASOTM>2.0.CO;2).
- Baringer, M.O., Price, J.F., 1999. A review of the physical oceanography of the Mediterranean outflow. *Mar. Geol.* 155, 63–82. [http://dx.doi.org/10.1016/S0025-3227\(98\)00141-8](http://dx.doi.org/10.1016/S0025-3227(98)00141-8).
- Barker, S., Knorr, G., Edwards, R.L., Parrenin, F., Putnam, A.E., Skinner, L.C., Wolff, E., Ziegler, M., 2011. 800,000 years of abrupt climate variability. *Science* 334 (80-), 347–351. <http://dx.doi.org/10.1126/science.1203580>.
- Bersch, M., Yashayaev, I., Koltermann, K.P., 2007. Recent changes of the thermohaline circulation in the subpolar North Atlantic. *Ocean Dyn.* 57, 223–235. <http://dx.doi.org/10.1007/s10236-007-0104-7>.
- Borenäs, K.M., Wåhlin, A.K., Ambar, I., Serra, N., 2002. The Mediterranean outflow splitting—a comparison between theoretical models and CANIGO data. *Deep-Sea Res. II Top. Stud. Oceanogr.* [http://dx.doi.org/10.1016/S0967-0645\(02\)00150-9](http://dx.doi.org/10.1016/S0967-0645(02)00150-9).
- Bryden, H.L., Stommel, H.M., 1984. Limiting processes that determine basic features of the circulation in the Mediterranean Sea. *Oceanol. Acta* 7, 289–296.
- Bryden, H.L., Candela, J., Kinder, T.H., 1994. Exchange through the Strait of Gibraltar. *Prog. Oceanogr.* [http://dx.doi.org/10.1016/0079-6611\(94\)90028-0](http://dx.doi.org/10.1016/0079-6611(94)90028-0).
- Cacho, I., Grimalt, J.O., Pelejero, C., Canals, M., Sierro, F.J., Flores, J.A., Shackleton, N., 1999. Dansgaard-oeschger and Heinrich event imprints in Alboran Sea paleotemperatures. *Paleoceanography* 14, 698–705. <http://dx.doi.org/10.1029/1999PA900044>.
- Cacho, I., Shackleton, N., Elderfield, H., Sierro, F.J., Grimalt, J.O., 2006. Glacial rapid variability in deep-water temperature and $\delta^{18}\text{O}$ from the Western Mediterranean Sea. *Quat. Sci. Rev.* 25, 3294–3311. <http://dx.doi.org/10.1016/j.quascirev.2006.10.004>.
- Cramp, A., O'Sullivan, G., 1999. Neogene sapropels in the Mediterranean: a review. *Mar. Geol.* 153, 11–28. [http://dx.doi.org/10.1016/S0025-3227\(98\)00092-9](http://dx.doi.org/10.1016/S0025-3227(98)00092-9).
- De Lange, G.J., Thomson, J., Reitz, A., Slomp, C.P., Speranza Principato, M., Erba, E., Corselli, C., 2008. Synchronous basin-wide formation and redox-controlled preservation of a Mediterranean sapropel. *Nat. Geosci.* 1, 606–610. <http://dx.doi.org/10.1038/ngeo283>.
- Elsanawany, R., Zonneveld, K., Ibrahim, M.I., Kholeif, S.E.A., 2010. Distribution patterns of recent organic-walled dinoflagellate cysts in relation to environmental parameters in the Mediterranean Sea. *Palynology* 34, 233–260. <http://dx.doi.org/10.1080/01916121003711665>.
- Hernández-Molina, F.J., Llave, E., Stow, D.A.V., García, M., Somoza, L., Vázquez, J.T., Lobo, F.J., Maestro, A., Díaz del Río, V., León, R., Medialdea, T., Gardner, J., 2006. The contourite depositional system of the Gulf of Cádiz: a sedimentary model related to the bottom current activity of the Mediterranean outflow water and its interaction with the continental margin. *Deep-Sea Res. II Top. Stud. Oceanogr.* 53, 1420–1463. <http://dx.doi.org/10.1016/j.dsr2.2006.04.016>.
- Hernández-Molina, F.J., Stow, D., Alvarez-Zarikian, C., Acton, G., Bahr, A., Balestra, B., Ducassou, E., Flood, R., Flores, J.A., Furota, S., Grunert, P., Hodell, D., Jiménez-Espejo, F., Kim, J.K., Kriisek, L., Kuroda, J., Li, B., Llave, E., Lofi, J., Lourens, L., Miller, M., Nanayama, F., Nishida, N., Richter, C., Roque, C., Pereira, H., Goñi Fernanda Sanchez, M., Sierro, F.J., Singh, A.D., Sloss, C., Takashimizu, Y., Tzanova, A., Voelker, A., Williams, T., Xuan, C., 2013. IODP expedition 339 in the Gulf of Cadiz and off West Iberia: decoding the environmental significance of the Mediterranean outflow water and its global influence. *Sci. Drill.* 16, 1–11. <http://dx.doi.org/10.5194/sd-16-1-2013>.
- Hernández-Molina, F.J., Llave, E., Preu, B., Ercilla, G., Fontan, A., Bruno, M., Serra, N., Gomiz, J.J., Brackenkridge, R.E., Sierro, F.J., Stow, D.A.V., García, M., Juan, C., Sandoval, N., Arnaiz, A., 2014. Contourite processes associated with the Mediterranean outflow water after its exit from the strait of Gibraltar: global and conceptual implications. *Geology* 42, 227–230. <http://dx.doi.org/10.1130/G35083.1>.
- Hernández-Molina, F.J., Stow, D.A.V., Alvarez-Zarikian, C.A., Acton, G., Bahr, A., Balestra, B., Ducassou, E., Flood, R., Flores, J.-A., Furota, S., Grunert, P., Hodell, D., Jiménez-Espejo, F., Kim, J.K., Kriisek, L., Kuroda, J., Li, B., Llave, E., Lofi, J., Lourens, L., Miller, M., Nanayama, F., Nishida, N., Richter, C., Roque, C., Pereira, H., Sanchez Goñi, M.F., Sierro, F.J., Singh, A.D., Sloss, C., Takashimizu, Y., Tzanova, A., Voelker, A., Williams, T., Xuan, C., 2014. Paleooceanography. Onset of Mediterranean outflow into the North Atlantic. *Science* 344, 1244–1250. <http://dx.doi.org/10.1126/science.1251306>.
- Hodell, D.A., Evans, H.F., Channell, J.E.T., Curtis, J.H., 2010. Phase relationships of North Atlantic ice-rafted debris and surface-deep climate proxies during the last glacial period. *Quat. Sci. Rev.* 29, 3875–3886. <http://dx.doi.org/10.1016/j.quascirev.2010.09.006>.
- Hodell, D., Crowhurst, S., Skinner, L., Tzedakis, P.C., Margari, V., Channell, J.E.T., Kamenov, G., MacLachlan, S., Rothwell, G., 2013. Response of Iberian margin sediments to orbital and suborbital forcing over the past 420 ka: Iberian margin paleoceanography. *Paleoceanography* 28, 185–199. <http://dx.doi.org/10.1002/palo.20017>.
- Iorga, M.C., Lozier, M.S., 1999. Signatures of the Mediterranean outflow from a North Atlantic climatology: 1 salinity and density fields. *J. Geophys. Res.* <http://dx.doi.org/10.1029/1999JC900115>.
- Jansen, J.H., Van der Gaast, S., Koster, B., Vaars, A., 1998. CORTEX, a shipboard XRF-scanner for element analyses in split sediment cores. *Mar. Geol.* 151, 143–153. [http://dx.doi.org/10.1016/S0025-3227\(98\)00074-7](http://dx.doi.org/10.1016/S0025-3227(98)00074-7).

- Kotthoff, U., Pross, J., Müller, U.C., Peyron, O., Schmiedl, G., Schulz, H., Bordon, A., 2008. Climate dynamics in the borderlands of the Aegean Sea during formation of sapropel S1 deduced from a marine pollen record. *Quat. Sci. Rev.* 27, 832–845. <http://dx.doi.org/10.1016/j.quascirev.2007.12.001>.
- Laskar, J., Fienga, A., Gastineau, M., Manche, H., 2011. La2010: a new orbital solution for the long-term motion of the Earth. *Astron. Astrophys.* 532, A89. <http://dx.doi.org/10.1051/0004-6361/201116836>.
- Lisiecki, L.E., Raymo, M.E., 2005. A Pliocene–Pleistocene stack of 57 globally distributed benthic $\delta^{18}O$ records. *Paleoceanography* 20, 1–17. <http://dx.doi.org/10.1029/2004PA001071>.
- Llave, E., Schönfeld, J., Hernández-Molina, F.J., Mulder, T., Somoza, L., Díaz Del Río, V., Sánchez-Almazo, I., 2006. High-resolution stratigraphy of the Mediterranean outflow contourite system in the Gulf of Cadiz during the late Pleistocene: the impact of Heinrich events. *Mar. Geol.* 227, 241–262. <http://dx.doi.org/10.1016/j.margeo.2005.11.015>.
- Llave, E., Hernández-Molina, F.J., Stow, D.A.V., Fernández-Puga, M.C., García, M., Vázquez, J.T., Maestro, A., Somoza, L., Díaz del Río, V., 2007. Reconstructions of the Mediterranean outflow water during the quaternary based on the study of changes in buried mounded drift stacking pattern in the Gulf of Cadiz. *Mar. Geophys. Res.* 28, 379–394. <http://dx.doi.org/10.1007/s11001-007-9040-7>.
- Maldonado, A., Nelson, C.H., 1999. Interaction of tectonic and depositional processes that control the evolution of the Iberian Gulf of Cadiz margin. *Mar. Geol.* 155, 217–242. [http://dx.doi.org/10.1016/S0025-3227\(98\)00148-0](http://dx.doi.org/10.1016/S0025-3227(98)00148-0).
- Martrat, B., Grimalt, J.O., Shackleton, N.J., de Abreu, L., Hutterli, M.A., Stocker, T.F., 2007. Four climate cycles of recurring deep and surface water destabilizations on the Iberian margin. *Science* 317, 502–507. <http://dx.doi.org/10.1126/science.1139994>.
- Meijer, P.T., Tüenter, E., 2007. The effect of precession-induced changes in the Mediterranean freshwater budget on circulation at shallow and intermediate depth. *J. Mar. Syst.* 68, 349–365. <http://dx.doi.org/10.1016/j.jmarsys.2007.01.006>.
- Millot, C., 2009. Another description of the Mediterranean Sea outflow. *Prog. Oceanogr.* 82, 101–124. <http://dx.doi.org/10.1016/j.poccean.2009.04.016>.
- Millot, C., 2014. Heterogeneities of in- and out-flows in the Mediterranean sea. *Prog. Oceanogr.* 120, 254–278. <http://dx.doi.org/10.1016/j.poccean.2013.09.007>.
- Millot, C., Candela, J., Fuda, J.-L., Tber, Y., 2006. Large warming and salinification of the Mediterranean outflow due to changes in its composition. *Deep-Sea Res. I Oceanogr. Res. Pap.* 53, 656–666. <http://dx.doi.org/10.1016/j.dsr.2005.12.017>.
- Mulder, T., Lecroart, P., Hanquiez, V., Marches, E., Gonthier, E., Guedes, J.-C., Thiébot, E., Jaaidi, B., Kenyon, N., Voisset, M., Perez, C., Sayago, M., Fuchey, Y., Bujan, S., 2006. The western part of the Gulf of Cadiz: contour currents and turbidity currents interactions. *Geo-Mar. Lett.* 26, 31–41. <http://dx.doi.org/10.1007/s00367-005-0013-z>.
- Myers, P.G., 2002. Flux-forced simulations of the paleocirculation of the Mediterranean. *Paleoceanography* <http://dx.doi.org/10.1029/2000PA000613>.
- Myers, P.G., Haines, K., Rohling, E.J., 1998. Modeling the paleocirculation of the Mediterranean: the last glacial maximum and the Holocene with emphasis on the formation of sapropel S₁. *Paleoceanography* 13, 586–606. <http://dx.doi.org/10.1029/98PA02736>.
- Nelson, C., Baraza, J., Maldonado, A., 1993. Mediterranean undercurrent sandy contourites, Gulf of Cadiz Spain. *Sediment. Geol.* 82, 103–131. [http://dx.doi.org/10.1016/0037-0738\(93\)90116-M](http://dx.doi.org/10.1016/0037-0738(93)90116-M).
- Nelson, C.H., Baraza, J., Maldonado, A., Rodero, J., Escutia, C., Barber, J.H., 1999. Influence of the Atlantic inflow and Mediterranean outflow currents on late quaternary sedimentary facies of the Gulf of Cadiz continental margin. *Mar. Geol.* 155, 99–129. [http://dx.doi.org/10.1016/S0025-3227\(98\)00143-1](http://dx.doi.org/10.1016/S0025-3227(98)00143-1).
- Richter, T.O., van der Gaast, S., Koster, B., Vaars, A., Gieles, R., de Stigter, H.C., De Haas, H., van Weering, T.C.E., 2006. The Avaatech XRF Core Scanner: technical description and applications to NE Atlantic sediments. *Geol. Soc. Lond. Spec. Publ.* 267, 39–50. <http://dx.doi.org/10.1144/GSL.SP.2006.267.01.03>.
- Rogerson, M., Rohling, E.J., Weaver, P.P.E., Murray, J.W., 2005. Glacial to interglacial changes in the settling depth of the Mediterranean outflow plume. *Paleoceanography* 20, 1–12. <http://dx.doi.org/10.1029/2004PA001106>.
- Rogerson, M., Rohlin, E.J., Weaver, P.P.E., 2006. Promotion of meridional overturning by Mediterranean-derived salt during the last deglaciation. *Paleoceanography* 21, PA4101. <http://dx.doi.org/10.1029/2006PA001306>.
- Rogerson, M., Rohling, E.J., Bigg, G.R., Ramirez, J., 2012. Paleoceanography of the Atlantic–Mediterranean exchange: overview and first quantitative assessment of climatic forcing. *Rev. Geophys.* 50, RG2003. <http://dx.doi.org/10.1029/2011RG000376>.
- Rosignol-Strick, M., 1985. Mediterranean quaternary sapropels, an immediate response of the African monsoon to variation of insolation. *Palaeogeogr. Palaeoclimatol. Palaeoecol.* 49, 237–263. [http://dx.doi.org/10.1016/0031-0182\(85\)90056-2](http://dx.doi.org/10.1016/0031-0182(85)90056-2).
- Sanchez Goñi, M.F., Harrison, S.P., 2010. Millennial-scale climate variability and vegetation changes during the last glacial: concepts and terminology. *Quat. Sci. Rev.* 29, 2823–2827. <http://dx.doi.org/10.1016/j.quascirev.2009.11.014>.
- Sankey, T., 1973. The formation of deep water in the Northwestern Mediterranean. *Prog. Oceanogr.* 6, 159–179.
- Schönfeld, J., 1997. The impact of the Mediterranean Outflow Water (MOW) on benthic foraminiferal assemblages and surface sediments at the southern Portuguese continental margin. *Mar. Micropaleontol.* 29, 211–236. [http://dx.doi.org/10.1016/S0377-8398\(96\)00050-3](http://dx.doi.org/10.1016/S0377-8398(96)00050-3).
- Schönfeld, J., 2002. A new benthic foraminiferal proxy for near-bottom current velocities in the Gulf of Cadiz, northeastern Atlantic Ocean. *Deep-Sea Res. I Oceanogr. Res. Pap.* 49, 1853–1875. [http://dx.doi.org/10.1016/S0967-0637\(02\)00088-2](http://dx.doi.org/10.1016/S0967-0637(02)00088-2).
- Schönfeld, J., Zahn, R., 2000. Late glacial to Holocene history of the Mediterranean outflow. Evidence from benthic foraminiferal assemblages and stable isotopes at the Portuguese margin. *Palaeogeogr. Palaeoclimatol. Palaeoecol.* 159, 85–111. [http://dx.doi.org/10.1016/S0031-0182\(00\)00035-3](http://dx.doi.org/10.1016/S0031-0182(00)00035-3).
- Shackleton, N.J., Hall, M.A., 1984. *Oxygen and Carbon Isotope Stratigraphy of the Deep Sea Drilling Project Hole 552A: Plio-Pleistocene Glacial History*. Initial Reports DSDP 81, pp. 599–609.
- Sierro, F.J., Flores, J.A., Baraza, J., 1999. Late glacial to recent paleoenvironmental changes in the Gulf of Cadiz and formation of sandy contourite layers. *Mar. Geol.* 155, 157–172. [http://dx.doi.org/10.1016/S0025-3227\(98\)00145-5](http://dx.doi.org/10.1016/S0025-3227(98)00145-5).
- Stow, D.A.V., Faugeres, J.-C., Gonthier, E., Cremer, M., Llave, E., Hernandez-Molina, F.J., Somoza, L., Diaz-Del-Rio, V., 2002. Faro–Albufeira drift complex, northern Gulf of Cadiz. *Geol. Soc. Lond. Mem.* <http://dx.doi.org/10.1144/GSL.MEM.2002.022.01.11>.
- Stow, D.A.V., Hernández-Molina, F.J., Alvarez-Zarikian, C., 2013. Expedition 339 summary. Exped. 339 summ. Proceedings of the Integrated Ocean Drilling Program <http://dx.doi.org/10.2204/iodp.proc.339.104.2013>.
- Thorpe, S.A., 1976. Variability of the Mediterranean undercurrent in the Gulf of Cadiz. *Deep Sea Res. Oceanogr. Abstr.* 23, 711–IN1. [http://dx.doi.org/10.1016/S0011-7471\(76\)80016-2](http://dx.doi.org/10.1016/S0011-7471(76)80016-2).
- Toucanne, S., Mulder, T., Schönfeld, J., Hanquiez, V., Gonthier, E., Duprat, J., Cremer, M., Zaragosi, S., 2007. Contourites of the Gulf of Cadiz: a high-resolution record of the paleocirculation of the Mediterranean outflow water during the last 50,000 years. *Palaeogeogr. Palaeoclimatol. Palaeoecol.* 246, 354–366. <http://dx.doi.org/10.1016/j.palaeo.2006.10.007>.
- Toucanne, S., Jouet, G., Ducassou, E., Bassetti, M.-A., Dennielou, B., Angue Minto'o, C.M., Lahmi, M., Touyet, N., Charlier, K., Lericolais, G., Mulder, T., 2012. A 130,000-year record of Levantine intermediate water flow variability in the Corsica trough, western Mediterranean Sea. *Quat. Sci. Rev.* 33, 55–73. <http://dx.doi.org/10.1016/j.quascirev.2011.11.020>.
- Voelker, A., Lebreiro, S., Schönfeld, J., Cacho, I., Erlenkeuser, H., Abrantes, F., 2006. Mediterranean outflow strengthening during northern hemisphere coolings: a salt source for the glacial Atlantic? *Earth planet. Sci. Lett.* 245, 39–55. <http://dx.doi.org/10.1016/j.epsl.2006.03.014>.
- Wang, Y., Cheng, H., Edwards, R.L., Kong, X., Shao, X., Chen, S., Wu, J., Jiang, X., Wang, X., An, Z., 2008. Millennial- and orbital-scale changes in the East Asian monsoon over the past 224,000 years. *Nature* 451, 1090–1093. <http://dx.doi.org/10.1038/nature06692>.
- Yamamoto, M., Sai, H., Chen, M.-T., Zhao, M., 2013. The East Asian Winter monsoon variability in response to precession during the past 150 000 yr. *Clim. Past* 9, 2777–2788. <http://dx.doi.org/10.5194/cp-9-2777-2013>.
- Zahn, R., Sarnthein, M., Erlenkeuser, H., 1987. Benthic isotope evidence for changes of the Mediterranean outflow during the late quaternary. *Paleoceanography* 2, 543–559. <http://dx.doi.org/10.1029/PA002i006p00543>.
- Ziegler, M., Lourens, L.J., Tüenter, E., Hilgen, F., Reichert, G.-J., Weber, N., 2010. Precession phasing offset between Indian summer monsoon and Arabian sea productivity linked to changes in Atlantic overturning circulation. *Paleoceanography* 25, PA3213. <http://dx.doi.org/10.1029/2009PA001884>.